HIGH PERFORMANCE MAGNETIC DEVICES BASED ON NANOCRYSTALLINE MATERIALS

Andrei MARINESCU[1], Horia GAVRILA[2], Ionel DUMBRAVA[3]

[1] ASTR Member, ICMET Craiova, [2] Correspondent Member ASTR, University Politechnica of Bucharest, [3] ICMET Craiova

Abstract: During the last two decades remarkable advances occurred in the field of semiconductor devices and smart systems, by their miniaturization and performance increase. Consequently, the reduction of equipment energy consumption and dimensions has resulted. A major contribution had here the new magnetic materials used, for instance, in the measurement technique, information technology and electric energy conversion. Starting from a precursor represented by amorphous magnetic materials, we assist now to the market success of nanocrystalline magnetic materials. Appeared for the first time in Japan and then developed by companies around the world, these materials have special properties for use at high frequency, don't utilize scarce and expensive chemical elements, have low losses and weights a.s.o. In this paper it is shown that the electric and electronic engineering fields can take full advantage of the features of these materials presented under different forms, from ribbons to thin films. After a brief presentation of the specific properties and a comparison with the classical magnetic materials, a series of applications such as wideband current/voltage transformers, disturbance filters and information recording systems are described, for which there are obtained smaller dimensions, wider frequency bands or greater storage capacities than until now. The results got by simulation and experiment, related to the development of some new high performance magnetic devices are presented.
Keywords: magnetic materials; nanocrystalline magnetic materials; specific properties; applications.

1. Introduction

We are all participating in a complex process of transforming the classical technologies for electricity generation, transmission and distribution within the framework of the smart grid conception [1]. Inclusion of unconventional distributed energy sources into the power systems and power circulation in both directions have imposed to increase the share of the energy conversion systems based on power electronics within the general effort of reducing the energy losses.

Magnetic materials are presented in all the forms of energy conversion, both in the traditional (power, distribution and instrument transformers) and in the modern ones, at which conversion takes place at high frequency for reducing the equipment dimensions, from the lowest power of the order of mW up to MW. It should be remarked the present preoccupations for reducing the losses generated at the power distribution in large urban agglomerations by using DC, which will lead to the increase of importance of power electronic based conversion systems [2].

Electrical power engineering development has been dominated since the beginning of 20th century by the FeSi alloy, for which successive developments have led to the reduction of magnetic loss of almost 10 times in the case of oriented crystal materials. Around 1910, NiFe (permalloy, mumetal etc) alloy, intended for the more and more frequent applications in radiotechnics appeared, under the form of thin ribbons, with reduced losses and high permeabilities, but saturation inductions of almost 3 times lower than in case of FeSi. The '50s bring a new material able to operate in practice at high frequencies; it is a ferrimagnetic material achieved by sintering some metallic powders (Mn, Ni, Zn etc) mixed with iron oxides, known under the generic name of ferrite, which dominated until now the market of magnetic materials for power electronics [3]. In the `70s, a new ferromagnetic material makes its appearance, this time an amorphous one (metallic glass) with trade name Metglas [4], which is a FeSi type alloy with small additions of B, Nb, Cu and sometimes Co, achieved by using the Rapid Solidification Tehnology - RST [5]. At present, amorphous magnetic materials find their applications both at industrial frequency and at high frequencies, being characterized by high permeabilities and low losses. Although quite used at the moment, they have an inherent metastability of the atomic state of metallic glass, process called "devitrification" that leads to loosing some mechanical and magnetic properties [6]. In the '90s, a new magnetic, nanocrystalline material [7] makes its appearance, as a result of the controlled devitrification of some amorphous alloys followed by different thermo-mechanical treatments, through which permeabilities similar to the basic amorphous material and losses similar to the ferritic materials could be obtained [8]. The

nano-structured magnetic materials represent domain of nanotechnologies with a fast development and a crucial role in the present and future energy conversion techniques, information technology and measurement technique. This brief review of the mentioned materials shows that the knowledge process closely linked to the above requirements follows the evolution of technical progress in which we are participating, so if between 1910 and 1950 (40 years) only developments of some known materials appeared, between 1950 and 1990 three new materials and research directions with fast application in practice appeared.
The paper aims to attract the attention of magnetic material users on the nanocrystalline material properties and applications. In the first part of it, the nanocrystalline material properties and applications in electrical and electronic engineering are described, and in the second part the applications of these materials to magnetic record of information are treated.

2. Nanocrystalline magnetic material

In 1988 the Japanese researchers Yoshizawa, Ogawa and Yamauchi patented and published [7] about a new class of ferromagnetic, magnetically soft and homogenous, ultrafine structure materials, resulted from an amorphous precursor under the form of thin ribbon. This alloy, at present called nanocrystalline, has a typical composition $(FeSi)_{89}(BNbCu)_{11}$ in atomic %. A widespread example is the alloy $Fe_{73.5}Cu_1Nb_3Si_{15.5}B_7$ produced in industrial quantities (more than 7000 tons in 2012) with the trade name of Finemet [9], Vitroperm [10], Nanophy [11] etc. The process through which an amorphous alloy is transformed into a nanocrystalline alloy may be briefly described as follows:

- in the first stage, the classical amorphous precursor with the same chemical composition as the future nanocystalline material is created by the RST method, which provides a high cooling rate of at least $dT/dt = 10^6$ K/s to avoid crystallization. The amorphous ribbon has the usual thickness of about 20 μm.
- in the second stage, the process of nano crystallization by annealing at a temperature of 500 – 540 °C during about 1 hour occurs, when the fast diffusion of Cu takes place leading to the appearance of FeSi crystalline germs with random crystallization directions, followed by the slow diffusion of Nb which inhibits the increase of grains at a typical nano level with the dimension D = 10 – 25 nm. The result of this controlled, stable "devitrification" is a soft magnetic material consisting in a nano crystalline phase of FeSi and a residual amorphous phase of about 30 % of the entire volume, material having special magnetic properties: relative permeability > 10^5 , a coercive field $H_c < 1$ A/m and very low saturation magnetostriction $\lambda_s \sim 10^{-6}$ [12].

This result is surprising within the framework of the classical magnetism theory [13], according to which the increase of grain dimensions in the macroscopic dimension range (D > 100 μm) leads to the lowering of H_c proportionally to 1/D and consequently the decrease of iron loss occurs. The decrease of the coercive field at the new nanocrystalline material was explained by Herzer within the random anisotropy model [14] as being proportional to D^6, like it results from Fig. 1.

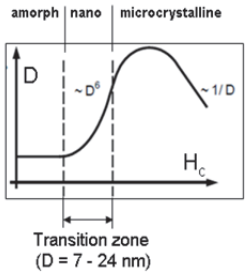

Fig. 1 Coercive magnetic field H_c depending on grain dimensions D [14].

The nanocrystalline materials occupy here the transition zone between the amorphous materials and the polycrystalline materials with magnetic properties comparable with the permalloy-type alloys or with Co-based amorphous alloys, but with higher saturation induction.
Similarly to the case of other magnetic materials, the hysteresis cycle may be changed by a uniaxial anisotropy induced during an annealing under magnetic field [15, 16]. But this process must take place under the final dimensional form (ready to use) of the magnetic circuit for which the manufacturer guarantees the magnetic properties (losses, Bs, Br/Bs etc), which until now was specific to sintered powder cores. Thus, the following types of magnetization cycles may be obtained [10] (Fig. 2):

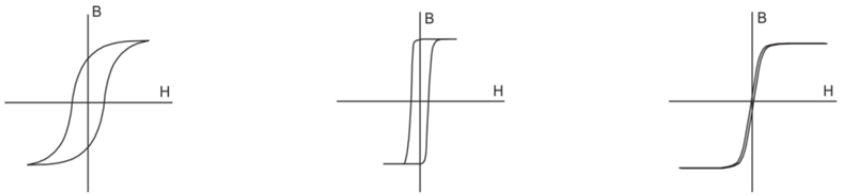

a) b) c)

Fig. 2. Typical magnetization cycles for a nanocrystalline material obtained by thermo-magnetic treatment (in finite state, for instance as toroid). a) **R** (round loop with $B_r/B_{sat} \geq 0.5$), b) **Z** (rectangular loop with $B_r/B_{sat} = 1$), c) **F** (flat loop with $B_r/B_{sat} \leq 0.1$).

The rounded cycle a), **R,** is obtained after the usual annealing without applying a magnetic field and is characterized by a very high initial permeability (μ_i =100000) and a very high maximum permeability (μ_{max} = 500000). The rectangular cycle b), **R,** is obtained by a thermo-magnetic treatment in which the annealing at a temperature below the Curie point is done simultaneously with the application of a longitudinal magnetic field (parallel with the ribbon axis). The initial permeability has a reduced value (μ_i = 5000) but the maximum permeability may reach values of ($\mu_{max} \geq 650000$). The flat cycle c), **F,** is achieved similarly to the case b) except that a magnetic field transverse to the ribbon axis is applied, the result being a hysteresis cycle with a constant slope and reduced remanence, i.e. a constant permeability ($\mu_i = \mu_{max}$) up to near saturation, so as depending on the strength of the applied field H, materials with different maximum permeabilities, from 1000 to 200000, could be obtained. The nanocrystalline materials with reduced permeabilities are a modern solution for avoiding the air gap practiced at the current transformers for protection (removal of saturation at high shortcircuit currents) [17]. Nanocrystalline cores are presented under toroidal or oval form in plastic box or molded in epoxy resin.

The main characteristics of a *nanocrystalline magnetic material found in industrial production* can be summarized as follows [9, 10, 11, 18]:

- Composition $Fe_{73.5}Cu_1Nb_3Si_{15.5}B_7$
- Magnetic saturation induction 1.2 T
- Resistivity ρ 120 μΩcm
- Magnetostriction λ_s < 0.5 ppm
- Coercive field H_c 0.5 A/m
- Density 7.35 g/cm3
- Material thickness d 15 - 20 μm
- Grain dimension D 10 - 17 nm
- Relative permeability μ_r 1000 - 200000
- Losses (0.3 T, 100 kHz, sinus) 80 W/kg *)
- Curie temperature 600 °C
- Operating temperature -40 to +120 (150) °C

*) A magnetic core with 1 kg weight may be used at a 20 kVA inverter.

3. Use of nanocrystalline cores at high frequencies

The above indicated data: resistivity, permeability, saturation induction and reduced losses make these materials to outperform all the materials used until now (ferrites, permalloy, amorphous materials) in low and high power applications at high frequency.

Further on, a comparison between the relative permeability (modulus) variation with frequency for a F-type [15, 19] nanocrystalline material and for a high quality Mn Zn ferrite [3] is done, as shown in Fig. 3. First, it can be noticed that at nanocrystalline materials, the relative permeability is at least an order of magnitude higher than at ferrites in the whole analyzed frequency range (10^{-3} – 10^3 MHz).

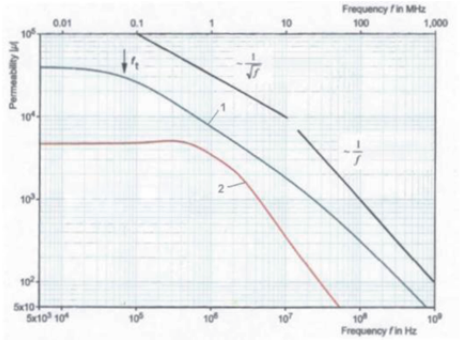

Fig. 3. Relative permeability modulus variation with frequency. 1 – nanocrystalline material, 2 - MnZn ferrite.

Conversely, the law of permeability variation with frequency is different for the two materials. At ferrites, the permeability remains constant up to near 1 MHz and then decreases due to the gyromagnetic effect, whose cutting frequency results from the relation [15]:

$$f_{gyro} = c \cdot \Gamma^* \cdot B_s/\mu_i \quad (1)$$

where $\Gamma^* = \Gamma/\mu_0 = 176$ GHz/T is the gyromagnetic ratio and $c \sim 1$ is a constant.
As a result, at ferrites the permeability decrease is proportional to 1/f.
At metallic materials, the permeability decrease starts from much lower frequencies, about 70 kHz in Fig. 3, being determined by the penetration depth Δ decrease with the frequency, given by the relation (2), where f_t is the cutting frequency of eddy currents given by the relation (3) [20]:

$$2\Delta = d\sqrt{f_t / f} \quad (2)$$

$$f_t = 4\rho/(\pi \cdot \mu_0 \cdot \mu_i \cdot d^2) \quad (3)$$

It results that beyond f_t the permeability modulus decrease is done proportionally to $1/\sqrt{f}$ (10 dB/decade) and only above10 MHz the frequency dependence becomes more pronounced, the decrease being proportional to 1/f (20 db/decade) similarly to the case of ferrites, as a consequence of the additional attenuation given by gyromagnetic effect [20].

4. Achieving an application: high frequency current transformer (HFCT)

HFCT is a wideband, high sensitivity CT able to reproduce accurately frequencies in a wideband of many decades or impulses with rise times of the order of ns and durations of the order of μs / ms encountered in modern electronics, without resonances and phase errors in the measuring frequency band and which introduces a constant insertion impedance in the measurement circuit.
The sensitivity (*S*) of a HFCT is defined in any point of the frequency characteristic as the ratio between the secondary voltage and primary current and is equivalent to a transfer impedance which, in general, is not a constant value [21]

$$S = \frac{U_2}{I_p} \quad [\Omega] \quad (4)$$

According to the application, *S* may vary within wide limits starting from 1 - 10 mV/mA for HFCTs used to measure the fast phenomena up to those utilized for measurements in power electronics, having much lower sensitivities, similar to the CTs used at low frequency in power grid, for which $S = 10^{-5}$ to 10^{-2} V/A.
A specific aspect related to the use of nanocrystalline materials is the possibility to change the magnetization characteristic by thermo-magnetic treatment and consequently to choose a material with ultra-linear magnetization characteristic and very reduced remanence, of F type, as it was shown in the previous paragraph. Such HFCT could be used both for low currents (mA) and for much higher currents (A) with no change, provided that the section of the conductor from the secondary winding and the burden are appropriately sized. This situation is described by the equality:

$$S = \mathbf{X}\ [\text{mV/mA}] \equiv \mathbf{X}\ [\text{V/A}] \quad (5)$$

In Fig. 4 it is presented the lumped parameters equivalent circuit of a HFCT in relation to the secondary, where the output voltage U_2 is obtained at the terminals of the burden R_2. For low values of R_2, typical to HFCTs, the use of lumped parameters is allowed also to very high frequencies [21]. The sensitivity frequency characteristic results from a relation of the type:

$$S(s) = \frac{U_2(s)}{I_p(s)} = \frac{Z_3(s)}{N} \cdot \frac{Z_1(s)}{Z_1(s) + Z_2(s) + Z_3(s)} \tag{6}$$

where Z_1, Z_2 şi Z_3 are the operational impedances of the component dipoles from the equivalent circuit, and N is the ratio of transformation.

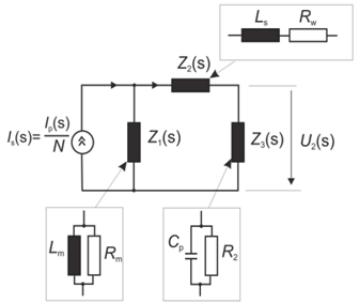

Fig. 4. Equivalent circuit of HFCT. $I_s(s)$ – current source in relation to secondary ($I_s = I_p / N$), $Z_1(s)$ – magnetization branch (inductivity and losses), $Z_2(s)$ – series branch (secondary winding resistance and leakage inductance), $Z_3(s)$ – output branch (parasitic capacitance and burden). Typical values: L_m = 1.7 mH, L_s = 100 nH, C_p = 20 pF, R_m =20 kΩ, R_w = 0.1 Ω, R_2 = 1 Ω.

After simple transformations, one gets:

$$S(s) = \frac{R_2}{N} \cdot \frac{sL_mR_m}{As^3 + Bs^2 + Cs + D} \tag{7}$$

representing the sensitivity frequency characteristic of a bandpass filter.
Analysis of this function leads to important practical relations for HFCT sizing, namely:
- Low limit frequency

$$f_{low} \cong R_2 / 2\pi L_m \tag{8}$$

- High limit frequency

$$f_{high} \cong 1/2\pi R_2 C_p \tag{9}$$

- Sensitivity in the passband where $\omega L_m >> R_2$, R_w, $\omega L_s << R_2$, $1/\omega C_p >> R_2$

$$S = R_2/N = Z_T \ [\Omega] \tag{10}$$

- Insertion impedance in the primary circuit

$$Z_{ins} = R_2/N^2 \ \ [\Omega] \tag{11}$$

- Frequency passband

$$BW = f_{high} - f_{low} \cong 1/2\pi R_2 C_p - R_2 / 2\pi L_m \tag{12}$$

Relation (10) may be applied only within mid frequency band and only if there the amplitude is constant; this is the rated value of the sensitivity S. Time-domain analysis should complete the above analysis for establishing the fidelity in reproducing the rectangular impulses, as it will shown further on.
Next, the characteristics of an electrostatically shielded HFCT achieved by the authors on the basis of the above considerations [22, 23, 24, 25] on a nanocrystalline toroidal magnetic core of F500 type [10] are presented. The frequency characteristics have been experimentally determined by a vector network analyzer (VNA) Anritsu MS 4630B and the results are given in Fig. 5a, compared with the results obtained by simulation, and a good compliance is noticed. On the basis of these characteristics, the following could be determined: frequency band, sensitivity, lower critical frequency and how to adjust it by means of the resistance R_2. The achieved HFCT has the following features:

PCT	Dimensions mm	S mV/mA	BW magnitude ± 3 dB
1	40 x 32 x 15	0.91	369.8 Hz – 14.4 MHz
2	100 x 80 x 20	0.497	25.1 Hz – 27.5 MHz
3	40 x 32 x 15	5.00	304.7 Hz – 6.56 MHz

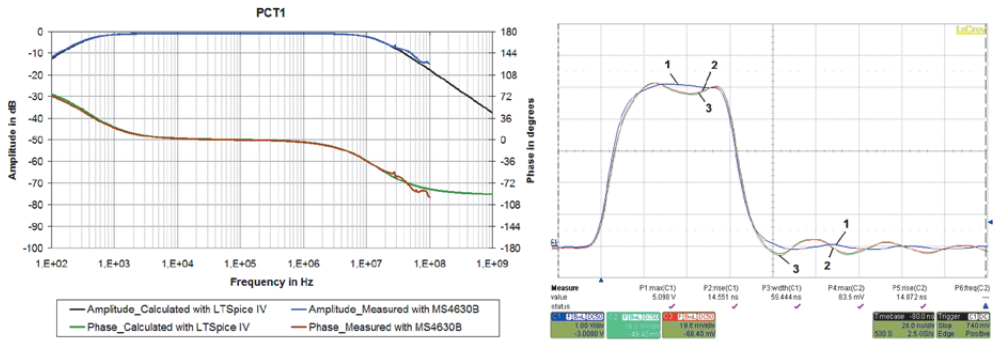

a) b)

Fig. 5. Frequency characteristics (experiment and simulation) and the time domain response of the achieved HFCT.

In Fig. 5b, the time domain response for unipolar rectangular impulses with duration of 60 ns similar to the impulses produced by PD is shown. The current impulse 1 is produced by a programmable impulse generator Agilent 33220A on a standard resistance of 50 Ω; the same current impulse is measured by a reference commercial HFCT (2) respectively by the achieved HFCT (3) with a digital oscilloscope LeCroy WaveSurfer 44MXs 400 MHz with 2.5 Gs/s. The rising and falling fronts of the three impulses are the same; the self oscillations visible on the impulses 2 and 3 are identical, confirming thus the quality of the developed HFCT.

The transformers of the above described type are currently in production of small series, as a result of the research undertaken in [22] within the framework of which a complex design algorithm was developed; this algorithm takes into account specific elements, such as the permeability variation with frequency for determining the drop rate at pulsed magnetization, figure of merit f x ΔB, metrological characteristics (range standardized only up to 200 kHz [26]), saturation current at which inductance decreases to 10 % of the initial value, extension of the product I x t by simultaneous DC demagnetization etc, elements that may be used also in other applications such as the disturbance filters or high frequency power transformers.

5. Other industrial applications

The potential industrial applications of the nanocrystalline magnetic materials with the indication of the type of material recommended to be used (**R, Z, F**) are presented further on:

- HF and Pulse wideband Current Transformers (CT) and Voltage Transformers (VT) - **F**
- HF power transformers (100 W up to 100 kW) and inductors for switched mode power supply, all types of inverters, X-ray generators and welding power sources a.s.o - **R, Z**
- 50 Hz current sensing for energy meters with DC acceptance - **F** and ground fault current interrupter - **R**
- Bulk-Current Injection (BCI) Probes for EMC - **R**
- EMC Filter for Common Mode and Normal Mode disturbances, mitigation of very fast transients and bearing currents in variable speed drives - **R, F**
- Power supplies for the Electrical Vehicles and Railway Transportation Systems - **R**
- Magnetic Energy Harvesting - **F**
- Testing and Monitoring systems - **R, F**
- Magnetic Recording

6. Magnetic recording media

One of the most important aplications of nanostructured magnetic materials is the modern recording media. The magnetic recording has known an accelerated progress, due to an accumulated know-how and to several findings in domains like material science, signal processing and recording technology [27-29]. One approaches the theoretical physical frontiers of the recording density, limits imposed by the energetically based assumptions concerning the thermal stability and the signal-to-noise ratio (SNR). Nevertheless, these limits can be overcome [30].

The main goals in magnetic recording are the continuous increase of the areal recording density and the highest possible signal-to-noise ratio (SNR).
With the conventional longitudinal magnetic recording, the maximum areal recording density has been assessed as physically limited to about 200 Gb/in^2. A further growth is limited by the superparamagnetic effect and by the limited possibilities to further improve writing heads design and pole materials in order to enhance the head writing field. To achieve higher recording densities, the classical pathway was to reduce the volume V of grains. But smaller it becomes, the energy KV of grains (K – anisotropy constant) becomes of the same order as the fluctuations of thermal energy, k_BT (k_B – Boltzmann' constant, T – temperature). Thus, to maintain acceptable values of the *factor of thermal stability*

$$\kappa = KV / k_BT \tag{13}$$

the media anisotropy must be increased. But in this case, the media coercivity can exceed the available field from the writing head existing today. For a good thermal stability of the grain, κ must be at least 60.
This is the famous *trilemma* of magnetic recording (thermal stability, media noise, and writability)!
Perpendicular magnetic recording has also made huge progress in the past few years, resulting in high-density commercial disk drive products, with areal density of more than 500 Gb/in^2 [31]. Nevertheless, there remain some important factors limiting its performance, as jitters that lower the SNR and, again, the super-paramagnetic effect. With the current values of these parameters, the conventional perpendicular recording (CPR) seems to be limited to a maximum density of about 1 Tb/in^2 [32].
Materials with an uniaxial magnetocrystalline anisotropy K_u of one order of magnitude higher than that of currently used Co-based alloys should be employed to achieve ultrahigh density recording medium. They are such materials. So, the $L1_0$ phase of FePt alloy is one of the most promising, due to its vey high value of K_u ($\cong$ 7 MJ/m^3), which leads to thermally stable grains with sizes down to 3-4 nm. But FePt films deposited at room temperature are magnetically soft, due to their metastable disordered structure and a high-temperature process must be used to obtain the fully ordered $L1_0$ structure of the films.
The writability problem can be solved using various assisting methods, including: domain-wall-, heat-, microwave- and precessional-assisted reversal methods.
Obviously, an alternative media architecture or recording schemes are needed to overcome these limits and several solutions have been proposed.

Patterned Media. Very promising are the recording media comprising monodisperse high-anisotropy nanoparticles in a self-organized patterning: (*bit*) *patterned media* (BPM) [33-38]. A (bit) patterned medium (BPM) is a very regular plane arrangement of discrete dots (islands, elements) of nanometric size, smaller than their critical monodomain size, and having a strong uniaxial magnetic anisotropy.
These media enable overcoming the superparamagnetic limit of the current thin-layer or granular media. They have higher thermal stability, low noise and higher signal resolution, which, in turn, led to higher recording density and a better SNR. A very important means of reducing the medium noise consists in eliminating the statistic fluctuations of the signal by using some magnetic grains very regular in point of size and layout, and magnetized in the same direction. The recording densities that can be thus achieved correspond to the minimum size of the thermally stable particles. For a current recording medium, a bit consists of many small magnetic grains magnetically isolated. Or, these grains can be easily switched by thermal energy even at ambient temperature if the grain size is further reduced in order to increase areal recording density.
Each bit is assigned to a dot magnetized longitudinally or, preferably, perpendicularly. This scheme is advantageous if the dots are monodomain, because the constraints of the writing and readout processes are then considerably reduced. The bits shape is determined not by the grain size, but by the configuration process of dots. Due to the monodomain character of each element, its recording is of the type "everything or nothing" (**1** or **0**), and the head need not be placed right above the bit. The major noise source of the recording process is no longer the media, but the method of locating and addressing individual particles. The transition noise, due to the magnetic coupling of the recorded bits, is eliminated. The SNR of the readout signal is much better due to the magnetic separation of the dots, thus to the absence of media noise and the excursion of transitions. The magnetic switching unit is large enough to prevent the thermal fluctuations and recording densities of some Tb/in^2 can be reached.
When designing a patterned medium, some requirements should be taken into account: (i) The dots must be arranged in a 2D template very regular. (ii) The material must have strong uniaxial anisotropy so that the dots are

monodomain and thermally stable. (iii) A narrow distribution of the switching field ensured by the very regular shape and size of the dots, as well as by the weakness of the magnetostatic interactions.
It is better for the easy axes of the grains to be aligned. With the circular disks this requirement is much easier to be fulfilled using materials with perpendicular anisotropy, which is easier to obtain as interfacial anisotropy. Crystalline or interfacial anisotropy patterned dots could be obtained by the physical configuration of Co-Pt multilayers, by depositing on configurated substrates, by modifying the Co-Pt or FePt alloys under the action of ion beams or by configuration with electron beams or focused ion beams of some thin CoCrPt layers.
The patterned media can be produced by an approach *top to bottom*, which implies producing the medium by sputtering and then patterning by lithography or implant with ion beam, either an approach *bottom to top*, using selective (dimensional) precipitations of monodomain particles from the solution or ordering them in very regular arrangements by self-assembling methods.
Various extensions of BPM allow using high anisotropy materials to improve the thermal stability and thus to facilitate the switching of dots with sufficiently low writing fields: exchange coupled composite dots or ledge elements (Fig. 6).
However, when the density of the magnetic dots approaches the limit of 1 Tdots/in^2, the recording performance of BPM can be seriously limited by the switching field distribution (SFD), which is due to intrinsic distributions of the media properties and to distribution of magnetostatic interactions between the recorded bits. A possible solution to improve this aspect is the ferromagnetic or antiferromagnetic coupling of magnetic dots (in any configuration represented on Figure 6) with a continuous low anisotropy film: this is the capped BPM (Fig. 7). In this structure the continuous capping layer reduces the dipolar interactions through lateral exchange interactions of neighboring bits, enabling also the reducing of SFD. There is now a large range of parameters that offer the possibility to optimize simultaneously SFD, thermal stability, and writability.

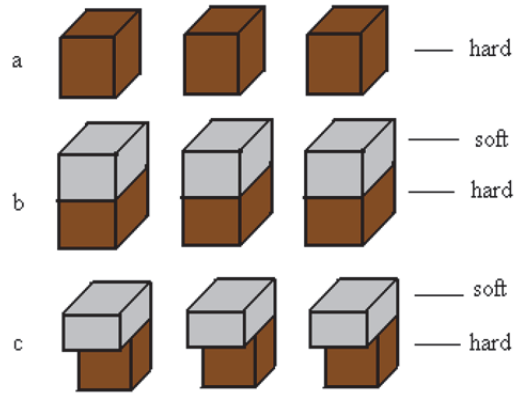

Fig. 6. Solutions for BPM:
a – homogeneous hard BPM;
b – exchange couples composite BPM;
c – ledge BPM.

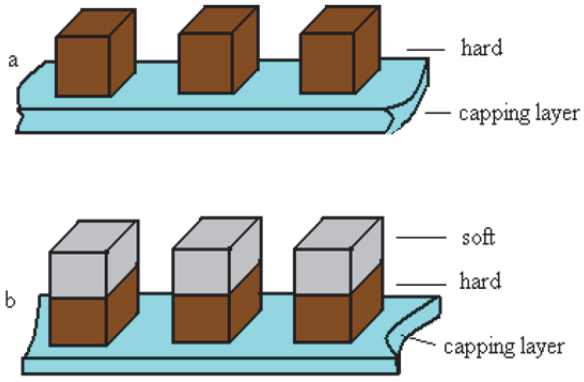

Fig. 7. Capped BPM: *a* – simple; *b* – composite.

There are two main methods of producing patterned media: lithographic techniques, the generation of *self-ordered magnetic arrays* (SOMA) or even a combination of these two approaches.
Concerning SOMA, there are some chemical reactions generating them or biologic materials forming a structure of high anisotropy monodisperse and monodimensional nanoparticles (of exactly the same shape and size). The chemically synthesized nanomagnets have size distributions extremely narrow, which favor the self-organized patterning, and enables potential densities of about 1 bit/particle, the equivalent of 10 – 50 Tb/in^2 (2 – 8 Tb/cm^2). SOMA media can serve as: conventional media with reduced dispersion; bit-patterned media with bit-transitions defined by rows of particles; and single-particle-per-bit recording media.
Among the materials having very strong anisotropy, special attention is given to the phase $L1_0$ of the equiatomic CoPt alloy and of the FePt alloy, thermally stable until grain diameters of 3 – 4 nm, which corresponds to a

uniaxial anisotropy constant $K_u = 5 \times 10^6$ J/m^3 and, respectively, 6.6×10^6 J/m^3. A self-assembled array of such particles shows well-aligned 2D close-packed nanostructures (Fig. 8).

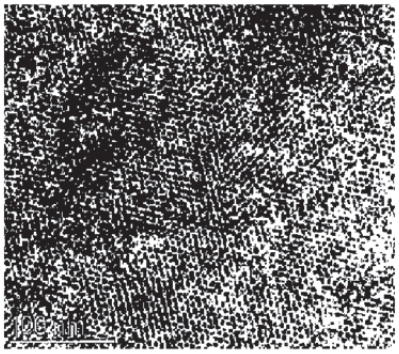

Fig. 8. TEM image of a self-organized *hcp* monolayer of protein-encapsulated nanoparticles.

In order to attain the forecast recording densities of some Tb/in^2, a strict control of the layer surface, of the uniformity of the composition, of thermal stability, of nanoparticles sizes, as well as of the orientation of their easy axes is required. If this control is not enough for refining of nanoparticles, one could use combined systems, for example the track patterning, by applying some grooves to strictly delimitate the tracks.

CGC Media. An important reason that impedes a complete valorisation of the potential of perpendicular recording is the granular nature of the media and thus the noise due to the irregularities of bit transitions. This noise is due to the intergranular exchange coupling, to the distribution of the anisotropy field and to the write field gradient. It can be reduced with the help of dense and uniform pinning sites. The intergranular exchange coupling is usually reduced as much as possible. But if this coupling is controlled by grain segregation, the increased thermal stability leads to a reduction of SNR. Thus an optimal value of the intergranular exchange coupling must be found, following from the tradeoff between SNR and thermal stability.
The solution is offered by the *coupled granular/continuous* (CGC) *media* [39]. A CGC medium is made up of a continuous layer C with a strong exchange coupling and without pinning centres, exchange coupled with a perpendicular granular layer G, both films being placed onto a soft magnetic underlayer (SUL) (Fig. 9). The small grains of the G layer, which are stable as a result of their coupling with the C layer, provide dense pinning centres for the walls in the C layer. The recorded transition has a usual structure in the G layer and a domain wall in the C layer. The transitions in the two layers overlap so that the C domain wall is pinned by the transition in the G layer and the transition of the CGC medium is given by the frontiers of the grains. Thus, the size of the unity switching is given by the size of the grains in the G layer, and the shape of the transitions at the surface of the CGC medium is given by the limits of the same grains. Moreover, the tendency to minimize the wall energy leads to some smoothening processes of the walls, the result being a supplementary reduction of media noise.

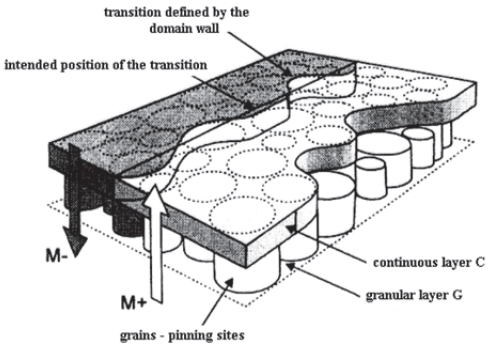

Figure 9. The principle representation of a CGC medium. The location of the domain wall (of the transition) in the C layer is imposed by the orientation of the grains magnetization in the G layer.

Both thermal stability and SNR can be improved by adjusting the structure and the parameters of the CGC media, because the exchange-coupled continuous layer, that achieve an *indirect* coupling of the grains of the G

layer, ensures a high thermal stability, while the granular host layer contributes to the reduction of the media noise and to improvement of the SNR of the written bits and of writability. The direct relationship between thermal stability and noise can be broken in a controlled way, thus evading the conventional limits of the recording density.
The CGC media use Co-Pt(Pd) multilayers or amorphous CoCrTb or Pt-rich CoCrPt alloy films or even CoCrPtB (these media are also called capped media or stacked media) for the continuous layer and CoCrX (usually CoCrPt) alloy films with weak lateral exchange coupling for the granular layer – but, in principle, the CGC concept may be extended to any continuous films pinned by an underlying granular film.
The CGC media structure is a path leading to percolated perpendicular media [41].

ECC Media. To solve the problem of low writability, a media structure, capable of low switching field without sacrificing the thermal stability, have been proposed: the *exchange coupled composite* (ECC) *media* [42], which exhibit only about half the switching field corresponding to conventional perpendicular media (CPM) for the same thermal stability. The potential advantages of these media are their poor sensitivity to the easy axis distribution, a better thermal stability, and a much higher recording density.
The *ECC* (or *composite perpendicular* or *exchange spring* or *domain-wall assisted) media* is a granular medium, in which each grain is made up of a magnetically soft lower region (1) and of a magnetically hard upper region (2), coupled by a positive exchange interaction (Fig. 10). Each composite grain is well exchange decoupled from its neighbouring grains, but the exchange coupling of the two regions of the same grain are very well controlled. The basic idea is that the soft magnetic part of the grain helps switch the hard magnetic part just near the switching point, while the thermal stability of the composite grain, ensured by the high value of the anisotropy constant of the hard region, is still unchanged, because the demagnetizing field in the hard part is much smaller than its switching field. Thus, the ECC media allow solving separately the problem of thermal stability and that of writing capability [43].
An entire fan of artificial magnetic structures can be then designed for ECC media.
The first one is a structure made up from a $[Co/PdSiO]_n$ multilayer as hard magnetic layer and a FeSiO soft magnetic layer, their exchange being controlled by the thickness of a thin Pt or PdSi interlayer. Quite useful is also the combination of hard CoPt alloys with an oxide to separate the grains and with an addition of Ni into this alloy to achieve the soft layer. A good structure is also a granular CoCrPt-SiO_2 thin film with a part of high Pt content as hard layer and a part of low Pt content as soft layer. The exchange decoupling of neighbouring grains is achieved through O_2 and Si doping, because SiO_2 tends to segregate to grain boundaries.

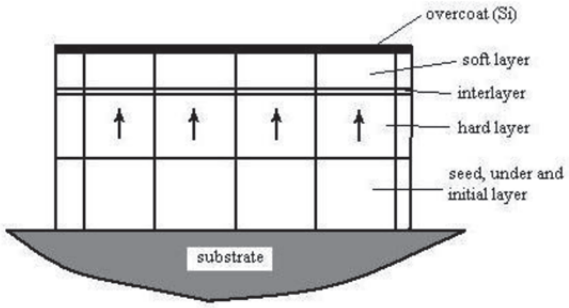

Fig. 10. Schematic representation of a possible structure of a ECC media.

The switching process in the ideal case is shown on Figure 11.
At $H = 0$, the energy minimum corresponds to the solutions (0,0) and (π,π), two stable states of the grain magnetization configuration: $\mathbf{M}_1$ and $\mathbf{M}_2$ both oriented $\uparrow$ (state **1**), respectively $\downarrow$ (state **2**). When applying a field $H \downarrow$, the energetic minimum (0,0) changes, pointing out the tendency of both magnetizations to be oriented according to this field. The switching field H_s is that value of the applied field for which this minimum disappears, the only energetic minimum corresponding to state **2**.
While the applied field is increased in the $\downarrow$ direction, the magnetization $\mathbf{M}_1$ of the soft region begins to rotate toward the in-plan direction (Fig. 11,b), thus leading to a drastic reduction of the average magnetization of the grain; the magnetization $\mathbf{M}_2$ of the hard region also rotates, but to an angle θ_2 smaller than θ_1.

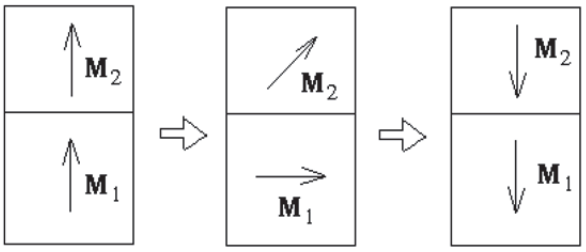

Fig. 11. The switching process in the optimal case with $V_1 = V_2$ and $M_1 = M_2$.

The role of this first step is that, due to the rotation of $\mathbf{M}_1$, the hard region of the grain is subjected to a *tilted* effective field, as result of the combined action of the applied field, the exchange field generated by the soft region and magnetostatic fields. Under the action of this tilted field, the magnetization $\mathbf{M}_2$ will switch more easily. At the critical point the hard part of the grain switches at a field that is about half of the original switching field. During the second step, under the action of a higher field, the rotation of both magnetizations continues, until their perfect ↓ orientation (Fig. 11,c). Due to this special switching mechanism, these ECC media are also named as *dynamic tilted media*.

The switching process of the ECC media is strongly dependent on the value of intragranular exchange coupling between the soft and the hard part of the grain. There is an optimum value of for the best switching performance of ECC media; it depends on the anisotropy contrast between the layers. The introduction of a sub-nanometric interlayer serves to tune the exchange coupling between the hard and the soft parts of grains. If this interlayer is missing and the intragranular exchange coupling is strong, we talk about *exchange spring media*.

ECC media had wider written tracks and slightly narrower erase bands than CPM, without any increase in adjacent track erasure. An increased intragranular exchange coupling increases the track width and narrows the erase band, resulting in sharper track edges. (The adjacent track erasure is today a key factor limiting recording density!) ECC media can solve the important problem of writability as well as other related effects and are capable to support areal recording densities beyond 1 Tb/in^2. A proper choice of materials used is a key requirement at this aim. So, materials with very high anisotropy constant must be used for the hard layers, as, for example, an optimised granular $L1_0$ phase of FePt or CoPt alloys or the *hcp* structured CoCrPtSiO layer with a high Pt content. For the magnetically soft layer, the FeCoSiO, FeNiSiO or NiSiO alloys can be used. A fine control of interlayer coupling and columnar growth of grains of very small diameter (few nanometers) are the main challenges to achieve the maximum benefits from the potential of ECC media.

It is evident that some basic aspects of ECC media and CGC media are similar [44] and this is the way to combine both structures in today practical recording media: a thin exchange coupled layer of low saturation magnetization was inserted between the too layers of a CGC medium to control the exchange coupling in vertical direction. Writing the media is then easier by increasing the lateral exchange by CGC effect or by decreasing the vertical exchange by ECC effect [45]; in the first case, the variation of the track width is more pronounced than in the second case, which is more advantageous to achieve higher track densities.

7. Conclusions

Magnetic materials are presented under all the forms of energy conversion, both in the traditional ones operating at industrial frequency and at the modern ones, at which conversion takes place at high frequency, having an important role in reducing the equipment dimensions and energy losses, from the lowest powers of the order of mW up to powers of the order of MW.

The paper aims at drawing the attention of the magnetic material users from Romania on the properties and applications of nanocrystalline materials that in the last two decades outperformed all the materials known up to present, both in some low and especially in medium and high frequency applications.

Starting from amorphous precursor, these materials represent a success of the international scientific research that penetrated rapidly in industrial practice, so as in 2012 the world production of such materials exceeded 7000 tons.

In the first part of the paper, the main properties of the nanocrystalline materials that occupy the transition zone between amorphous materials and polycrystalline materials with magnetic properties comparable with the permalloy – type alloys or with amorphous materials, but with higher saturation induction are presented.
By thermo-magnetic treatments, the form of the hysteresis cycles (R, Z, F) can be changed for adapting them to different applications. Among these, the F (flat) characteristic, an ultra-linear one in which the permeability remains constant up to near saturation, attracts the attention.
As compared to the high quality ferrites, the nanocrystalline materials have a permeability of at least one order of magnitude higher, within a frequency range between 10^{-3} and 10^{3} MHz.
It is presented in detail the achievement of some high frequency current transformers (HFCT), an important application to control the frequency inverters.
There are indicated the fields in which the nano-structured materials bring or will bring a major contribution.
Because these materials do not contain rare or expensive metals (Ni, Co etc,) their price decreases continuously simultaneously with the increase of the number of applications and users.

References

[1] X. Yu, C. Cecati, T. Dillon, M. G. Simoes, The New Frontiers in Smart Grids - An Industrial Electronics Perspective, IEEE Industrial Electronics Magazine, pp. 49-63, September 2011.
[2] Q. Huang, Y. Song, X. Sun, L. Jiang, P. W. T. Pong, Magnetics in Smart Grid, *IEEE Trans. Magn.*, vol. 50, no. 7, paper 0900107, 2014.
[3] EPCOS, "Ferrites and Accessories" Data Book, 2013, Available online: www.epcos.com
[4] Available online : www.metglass.com
[5] A. M. Leary, P. R. Ohodnicki, M. E. MCHenry, Soft Magnetic Materials in High-Frequency, High-Power Conversion Applications, JOM, Vol. 64, , pp 772-781, 2012.
[6] Herzer, Grain size dependence of coercivity and permeability in nanocrystalline ferromagnets, *IEEE Trans. Magn.*, vol. 26, no. 5, pp. 1397-1402,1990.
[7] Y. Yoshizawa, S. Oguma and K. Yamauchi, "New Fe-based soft magnetic alloys composed of ultrafine grain structure", J. Appl. Phys., vol. 64, pp. 6044-6046, 1988.
[8] G. Herzer, Nanocrystalline soft magnetic materials, Physica Scripta Vol T49A, pp. 307-314, 1993.
[9] Available online : www.hitachi-metals.co.jp
[10] Available online : www.vacuumschmelze.com
[11] Available online: www.imphi.fr
[12] G. Herzer, Grain Structure and Magnetism of Nanocrystalline Ferromagnets, *IEEE Trans. Magn.*, vol. 25, No. 5, pp. 3321-3329,1989.
[13] R.M. Bozorth, Ferromagnetism, 968 pp., IEEE Press Classic Reissue, ISBN 0-7803-1032-2, 1993.
[14] G. Herzer, Nanocrystalline soft magnetic alloys. In: K.H.L. Buschow (Ed.), *Handbook of Magnetic Materials*, Vol. 10, Elsevier, Amsterdam, 1997.
[15] R. Hilzinger, W. Rodewald, "Magnetic Materials", Publics Publishing, Erlangen, 2013.
[16] Y. Yoshizawa and K. Yamauchi, "Induced magnetic anisotropy and thickness dependence of magnetic properties in nanocrystalline alloy finemet", *IEEE Trans. Magn.*, vol. 5, no. 6, pp. 1070–1076, 1990.
[17] J. Petzold, "Applications of nanocrystalline softmagnetic cores in modern electronics"; In: Soft Magnetic Materials 16 (09.-12.09.2003), Vol. 1, page 97.
[18] Available online : www.magnetec.de
[19] R. Wengerter, "Nanocrystalline soft magnetic cores" 16 pp., Available online: www.sekels.com
[20] J. Beichler, "Designvorteile durch nanokristalline Kerne", *E&E Kompendium 2005/2006*, page 112-114.
[21] A. Marinescu, I. Dumbravă, "Nano-Crystalline Magnetic Core Pulse CT Development and Assessment for Partial Discharge Measurements", 2014 International Conference on Applied and Theoretical Electricity (ICATE), Craiova, 23 - 25 Oct 2014.
[22] Scientific Programme PN 09010118 funded of Romanian Ministry of Research.
[23] A. Marinescu, I. Dumbravă, "Lightning impulse testing of power transformers using HFCT's", ARWtr2013 Advanced Research Workshop on Transformers, Baiona, Spain, 28 - 30 October 2013.
[24] A. Marinescu, I. Dumbravă, "Measurement of winding currents during impulse testing of power transformers. Shunts vs. Inductive", 18th International Symposium on High Voltage Engineering ISH-2013, Seoul, Korea, August 25nd - 30th 2013.

[25] I. Dumbravă, A. Marinescu, I. Badea, M. Boruz, D. Popa, L. Vlădoi, "Power Transformer LI Tests with High Frequency Pulse CTs for Current Measurement", 2014 International Conference on Applied and Theoretical Electricity(ICATE), Craiova, 23 - 25 Oct 2014.
[26] IEC/EN-60404-6, 2003 "Method of measurement of the properties of magnetically soft metallic and powder materials at frequencies in the range 20 Hz to 200 kHz by the use of ring specimens".
[27] S.X. Wang and A.M. Tartorin, Magnetic Information Storage Technology, Academic Press, Nw York – London, 1999.
[28] P. Ciureanu and H. Gavrilă, Magnetic Heads for Digital Recording. Elsevier, Amsterdam, 1990.
[29] H. Gavrilă, Magnetic Recording (in Romanian). Printech, Bucharest, 2005.
[30] D. Weller and A. Moser, I.E.E.E. Trans. Magn. 35, 4423 (1999).
[31] T. Osaka, M. Datta, and Y. Shachan-Diamond, « Electrochemical nanotechnologies », in: Nanostructure Science and Technology, New York, Springer, 2010, pp.113-129.
[32] Y. Shiroishi, K. Fukuda, I. Tagawa, H. Iwasaki, S. Takenoiri, H. Tanaka, H. Mutoh, and N. Yoshikawa, I.E.E.E. Trans. Magn. 45, 3816 (2009).
[33] R.M.H. New, R.F.W. Pease, and R.L. White, J. Vac. Sci. Technol. B12, 3196 (1994).
[34] S.Y. Chou, P.R. Krauss, and L. Kong, J. Appl. Phys. 79, 6101 (1996).
[35] H. Gavrila, J. Optoelectronics Adv. Mater. 6, 891 (2004).
[36] V. Parekh, C.E A. Ruiz, B. Craver, J. Wolfe, and D. Litvinov, Nanotechnology 17, 2079 (2006).
[37] H. Gavrila, J. Optoelectronics Adv. Mater. 10, 757 (2008).
[38] B.D. Terris, M. Albrecht, G. Hu, T. Thomson, and C.T. Rettner, I.E.E.E. Trans. Magn. 44, 2822 (2008).
[39] Y. Sonobe, D. Weller, Y. Ikeda, K. Takano, G. Zeltzer, B.K. Yen, M.E. Best, *J.M.M.M*. 235, 424 (2001).
[40] Y. Sonobe, K. K. Tham, T. Umezawa, C. Takatsu, J. A. Dumaya, P.Y. Leo, *J.M.M.M*. 303, 292, 2006.
[41] J. Zhu, Y. Tang, *J. Appl. Phys*. 99, 2006.
[42] R. H. Victora and X. Shen, I.E.E.E. Trans. Magn. Vol. 41 (2005), p. 537.
[43] J. P. Wang, W. K. Shen, and S.-Y. Hong, I.E.E.E. Trans. Magn. Vol. 43 (2007), p. 682.
[44] H. Gavrila, Proc. of the Romanian Academy, Series *A*, Vol. 11 (2010), p. 41.
[45] H. J. Richter, G. Choe, and B. D. Terris, I.E.E.E. Trans. Magn. Vol. 47 (2011), p. 4769.